

Reconstruction of Air-Shower Parameters through Lateral Distribution Function of Ultra-High Energy Particles

KADHOM F. FADHEL^{a,b,*} AND A.A. AL-RUBAIEE^a

^a*Department of Physics, College of Science, Mustansiriyah University, Palestine St., P.O. Box 14022, Baghdad, Iraq*

^b*Directorate General of Education in Diyala, Ministry of Education, Iraq*

Doi: [10.12693/APhysPolA.140.344](https://doi.org/10.12693/APhysPolA.140.344)

*e-mail: kadhmfakhry@uomustansiriyah.edu.iq

Scientific interest in interactions of ultra-high energy cosmic rays stimulated these simulation studies. Different hadronic interaction models (such as SIBYLL, EPOS, and QGSJET) were simulated using air showers simulation AIRES program (version 19.04.00). Also, the charged particle density of extensive air showers was calculated by estimating the lateral distribution function. Simulation of the two primary particles (iron nuclei and protons) was performed, taking into account their primary energy effect as well the zenith angle for charged particles produced in the extensive air showers, within the energy range 10^{17} – 10^{19} eV. At extremely high energies (10^{17} eV, 10^{18} eV, 10^{19} eV) new parameters were obtained as a function of the primary energy, by fitting the lateral distribution curves of extensive air showers using the sigmoidal function (logistic model). Comparison of the results showed good agreement between the values obtained with the parameterized lateral distribution sigmoidal function and the experimental results from AGASA Extensive Air Showers observatory. The comparison was made for the primary protons as well as iron nuclei, with the production of electron–positron pairs and charged muons as secondary particles at energy of about 10^{19} eV and $\theta = 0^\circ$.

topics: cosmic rays, extensive air showers, lateral distribution function, AIRES system

1. Introduction

The investigation of the characteristics of extensive air showers (EAS) that were triggered by ultra-high energy cosmic rays (CRs) is crucial [1]. Note that the EAS chain reaction detects high energy CRs produced in the surrounding atmosphere. Since certain primary particles are undetectable directly, they must be investigated indirectly, based on the showers, and measured in different ways [2]. When a high-energy CRs particle collides with an atom in the atmosphere surrounding the Earth, a shower of secondary particles is generated, which further interact and generate more secondary particles before they reach Earth's surface [3]. The primary properties of cosmic ray must be deduced from the particles and their ratios in the shower, and from the creation of a shower in the atmosphere [2].

It should be mentioned that this study provides a unique insight into the cascade phenomena that are due to the interaction of CR with the nuclei of atmospheric atoms. Such interactions can give much higher energy than those obtained in man-made collisions in the high-energy interaction characteristics of hadrons [3]. A simple analytical model cannot

thoroughly explain the comprehensive creation of showers because the process of interaction is too complicated [4]. The shower reaction, often called a cascade, continues until the average energy possessed by the single and multiple particles drops below their critical energy. This criterion is often lost due to multiple collisions rather than other radiative processes [5]. Therefore, Monte Carlo (MC) simulation is normally used to model each individual shower particle transport and interaction, based on our current understanding of interactions, decays, and particle transport in matter [6]. Because of the complexity of reactions involved during the formation an air shower, numerical simulations are often used to conduct comprehensive studies of its characteristics. This affects both simulation of the interactions of particles and transport in the atmosphere, as well as the model assumptions affect quantitative results [7]. All of the processes that have a major impact on the shower actions such as all the electrodynamic interactions, hadronic collisions, photonuclear processes, particle decays, and so on [8], must be taken into account by simulating algorithms. The density of charged particles as a function of the primary energy of particles is seen in the current calculations.

The simulation of the LDF was performed by the AIRES program of primary particles (iron nuclei and protons) in the energy range 10^{17} – 10^{19} eV for two different zenith angles, i.e., 0° and 10° . At angles above 10° the effects become rather complicated or non-significant due to many path-variation possibilities. The LDF of secondary particles in the production of electron–positron pair and muons was simulated. Through the sigmoidal function (logistic model) new parameters were obtained for LDF, i.e., the dependence of densities of particles produced in EAS on the primary energy of particles within the energy spectrum range of 10^{17} – 10^{19} eV.

The comparison of the results showed a good agreement between (i) the estimated LDF of charged particles and (ii) the data from AGASA EAS observatory as well as (iii) the simulated results of Sciutto et al. [8] at 10^{19} eV. For similar works, either a new equation or new parameters are deduced in calculating the (LDF), or, they are dependent on the Nishimura–Kamata–Greisen (NKG) function. The novelty in this paper is obtaining a new function $K(E)$ by developing a sigmoidal function which depends on four parameters as a function of the primary energy.

2. The lateral distribution function

The density of the charged particles for different distances from the central position is one of the basic EAS important through large ground-based air shower arrays can be calculated very accurately. Since the detection of the EAS, the lateral or radial density distributions $\rho(r)$ of various types of particles generated in EAS have been focused for experimental and theoretical researches [9, 10]. The right lateral distribution function (LDF) of EAS muons and electrons is crucial for EAS research and study. The problem of quick LDF calculations that are both correct and adequate to the experimental data at very large distances from the shower axis ($r \geq 1$ km), has yet to be solved. Therefore, the analysis of experimental data on giant air showers and the design of new experiments, reliable results over such large distances are needed [11].

The most widely used method for super-high energy EAS simulation gives an empirical overview of electromagnetic sub-showers based on various modifications. Therefore, the reconstruction of a shower core as well the shower path, knowledge of the LDF is essential. It can also be compared to model calculations for the primary mass details and therefore give useful information. For a variety of reasons, the EAS lateral distribution is critical for the air shower phenomenon [12]. The first is that the energy and mass of the primary particle can be calculated and it is the most important among the numbers, and also the distribution of ground particles can be found. To connect the observables to the primary energy as well as mass, more accurate algorithms need comprehensive air shower simulations [13].

LDF is the shower characteristic of the cascade at different heights in Earth’s atmosphere [14]. The Nishimura–Kamata–Greisen (NKG) function is a commonly used term to describe the LDF type [15], and it is expressed via

$$\rho_e(R) = \frac{N_e C(s)}{2\pi R_M^2} \left(\frac{R}{R_M}\right)^{s-2} \left(\frac{R}{R_M} + 1\right)^{s-4.5}, \quad (1)$$

where $\rho_e(R)$ is the electrons surface density [particle/cm²] at the distance R from the shower core, N_e is the total number of electrons in the shower, R_M is the Molière radius at the sea level ($R_M = 78$ m). The Molière radius is a material characteristic constant, its value depends on both the radiation length (X) and the atomic number (Z) based on the approximate relation

$$R_M = 0.0265X(Z + 1.2). \quad (2)$$

The scale of perfectly contained electromagnetic showers that are triggered using electrons or photons with high energy can be specified. By reducing the Molière radius, the shower position can be more accurately resolved. Therefore, R_M is crucial in the field of experimental particle physics for the calorimeters design. Finally, s is the shower age parameter where the NKG-function is valid for the range $0.8 < s < 1.6$, and $C(s)$ is the normalizing factor equal to $0.366(2.07 - s)^{1.25} s^2$ [16].

3. Results and discussion

3.1. AIRES simulations

The specifics of shower evolution are extremely complicated to be completely delineated by uncomplicated analytical modeling. In addition, the MC simulation of interaction and transport of every single particle is needed to execute modeling of shower evolution. Lately, MC packages are employed for simulating EAS using AIRES (AIR shower Extended Simulation) system [4]. Various hadronic interaction models are utilized for these event generators, such as SIBYLL [17], QGSJET [18] and EPOS [19]. Therefore, the air shower simulation programs are made up of a variety of interconnected procedures that run on a data set with a variable number of records, changing the content and increasing or decreasing the size of the data set according to predetermined laws. Internal control procedures in AIRES’ simulation engine continuously check and report particles touching the ground and/or moving over the predetermined observation surfaces between the ground and injection stages. The number of showers is determined and then the identity of the elementary particle is determined, as well as its energy which can interact with atoms of the atmosphere. Then we define the name of the task, as well as the kinetic energy of electrons, muons, and gamma rays. Next, we define the thinning energy and the zenith angle, and then choose the observing levels for the array to

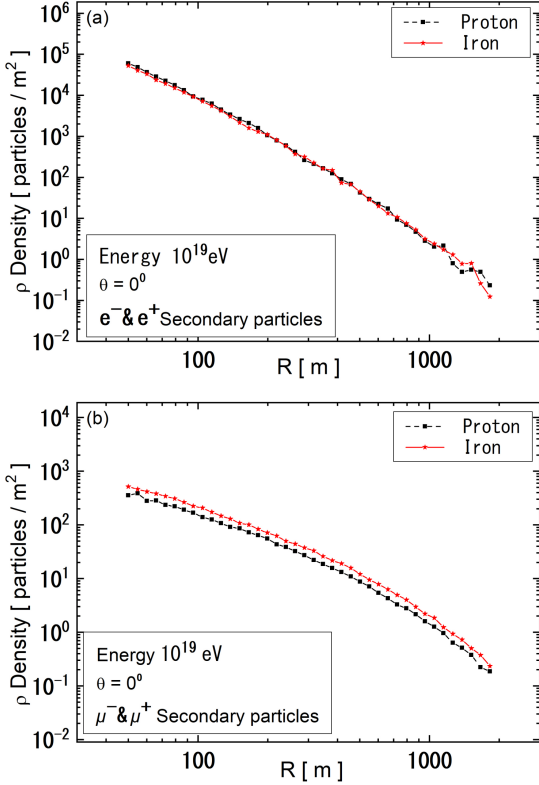


Fig. 1. The relation between $\rho(r)$ and distance from simulation of the LDF by AIRES system for the primary proton as well iron nuclei at vertical showers.

be used. Finally, we define the name of the secondary particles resulting from the chain reaction. The diffractive interactions possess a straight influence on the shower progress. Also, this fact is clearly confirmed by graphing the densities of showers versus the shower core of the atmosphere at certain value of energies of 10^{17} , 10^{18} , and 10^{19} eV. The results were plotted depending on the data incoming from simulations executed via the AIRES system for assorted hadronic interaction models (SIBYLL, QGSJET and EPOS). The simulation was employed to investigate the production of primary particles (protons as well the iron nuclei) resulting from air showers within the range of primary energy 10^{17} – 10^{19} eV and explored the LDF growth of various hadronic interaction models created by subsequent primary CRs of the extremely high value of energy reacting with the atmosphere and organized overall correlated production data [4]. The whole simulation process is executed via the AIRES system which benefited from the use of the thinning level 10^{-6} relative.

In Fig. 1, we present the difference between the primary LDF proton and iron nuclei at initial energy 10^{19} eV and vertical EAS showers for two secondary particles ((a) the production of the electron-positron pair and (b)) charged muons as secondary particles.

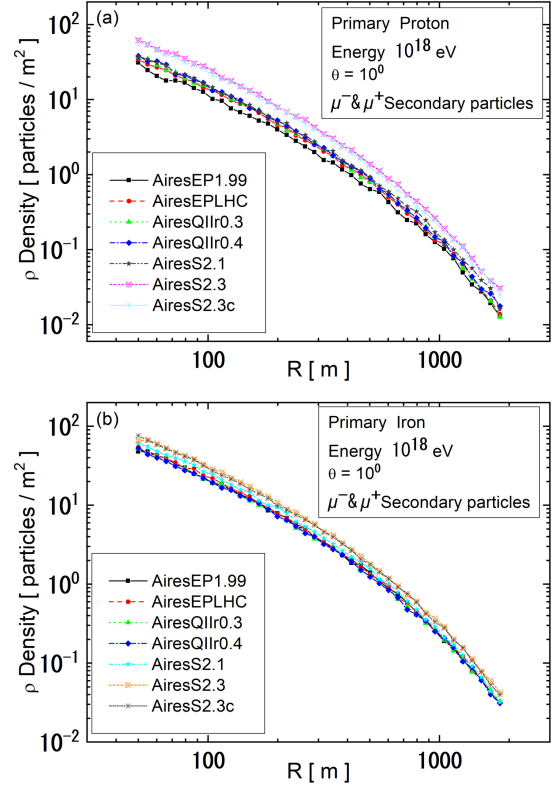


Fig. 2. Comparison with different hadronic interaction models like (SIBYLL, QGSJET, and EPOS) by using AIRES system of LDF at the primary energy 10^{18} eV for secondary muons.

In Fig. 2, the simulation results are shown for LDF using AIRES systems for different hadronic interaction models (SIBYLL, QGSJET, and EPOS) for the primaries ((a) protons as well iron nuclei (b)) at fixed energy of 10^{18} eV and inclined zenith angle $\theta = 10^\circ$, for muons secondary particles.

3.2. Parameterization of LDF

The Aires simulation was applied for the primary protons as well iron nuclei within the energy range 10^{17} – 10^{19} eV and explores the LDF for different hadronic models. The sigmoidal function (logistic model) was used to parameterize the LDF of showers that started in EAS, yielding four parameters for various primary particles, the function is denoted by

$$\rho(E) = \frac{\eta - \zeta_c}{1 + \left(\frac{x}{\delta}\right)^\alpha} + \zeta_c, \quad (3)$$

where ρ is the density of EAS shower as a function of the primary energy E , while η , ζ_c , δ , α are coefficients for LDF (see Table I). These coefficients are obtained by fitting the AIRES results, which are given by the polynomial

$$K(E) = a_0 + a_1 E + a_2 E^2, \quad (4)$$

where $K(E)$ represents the parameters η , ζ_c , δ , α of (3), being a function of the primary energy with a_0 , a_1 and a_2 as their coefficients (see Table I).

TABLE I

Coefficients of the sigmoidal function (logistic model) (3) used with the parameterized AIRES program simulation for the primaries proton as well iron nuclei within the energy range of 10^{17} – 10^{19} eV and two zenith angles $\theta = 0^\circ$ and 10° .

Primary particles	Secondary particles	$K(E)$ [eV]	Coefficients		
			a_0	a_1	a_2
p	$e^- \& e^+$	η	118.86495	1849.60556	26485.14832
		ζ_c	-0.9945	-27.25218	-142.30949
		δ	86.23676	59.78296	46.00644
		α	1.33741	1.21566	1.34987
	$\mu^- \& \mu^+$	η	2.26595	21.77746	153.23286
		ζ_c	0.82059	8.07847	40.86455
		δ	1253.03081	1094.68689	1101.96244
		α	8.18762	7.46504	6.00806
Fe	$e^- \& e^+$	η	114.98125	1468.11536	23410.17673
		ζ_c	-0.86126	-24.80306	-208.61533
		δ	83.17814	80.39021	49.32528
		α	1.26734	1.28711	1.2592
	$\mu^- \& \mu^+$	η	3.29002	26.11111	217.12133
		ζ_c	1.20671	9.54119	68.42865
		δ	1169.71658	1102.07871	1102.75785
		α	7.08781	6.27649	6.43017

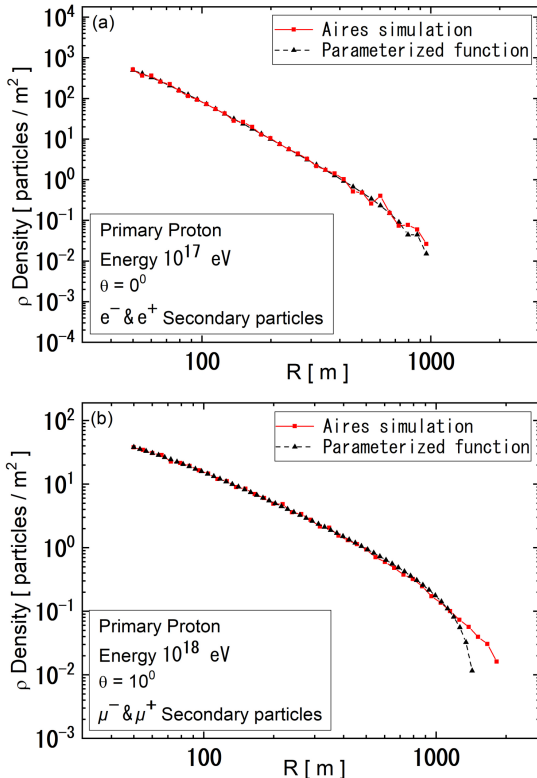


Fig. 3. Lateral distribution simulated with AIRES system (solid lines) and one calculated with (3) (scattered) for primary proton (a) at energies 10^{17} within the production of the electron–positron pair, and (b) within the production of the muons charged secondary particles at energies 10^{18} eV.

In Table I, the parameter ζ_c has a negative values for $e^- \& e^+$ because the function tends to have minimizing trend which affects the shower density. Also it was noted that η for $e^- \& e^+$ and $\mu^- \& \mu^+$ have large values for all cases. It is worth to note that η for $e^- \& e^+$ and $\mu^- \& \mu^+$ have large values for all cases.

In Fig. 3, we present the simulation of LDF using the AIRES system for different hadronic interaction models (SIBYLL, QGSJET, and EPOS). The results are devoted to the primaries (protons as well iron nuclei) at fixed energy of 10^{18} eV and inclined zenith angle of $\theta = 10^\circ$, and the muons charged secondary particles.

The parameterization of the shower density in EAS of primary energy is made for two primary energies 10^{17} and 10^{18} eV and two zenith angles 0° and 10° at the production of the electron–positron pair and muons secondary particles. The error ratio was 0.9935% and 0.9974%, respectively, for $e^- \& e^+$ and $\mu^- \& \mu^+$. These results are satisfactory. We can consider that the sigmoidal function (logistic model) applies well both to electrons and muons.

3.3. The comparison with AGASA observatory

The parameterized LDF obtained with the sigmoidal function (3) was compared with the experimental results for the AGASA array [20]. As shown in Fig. 4, the comparison gave good compatibility for both primaries iron nuclei as well protons with the fixed primary energy 10^{19} eV for vertical EAS showers that initiated muons as secondary

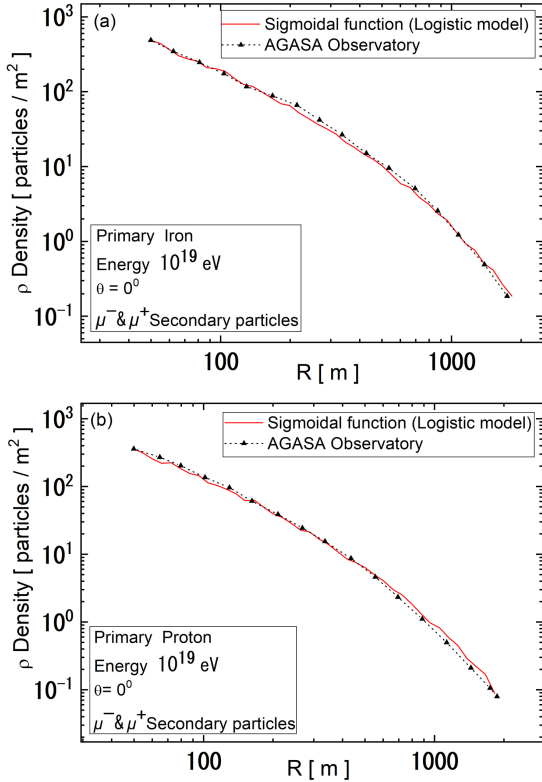


Fig. 4. Comparison of the parameterized LDF obtained using (sigmoidal function) with the experimental results by AGASA array for the primary ((a) iron nuclei and (b) proton) at the energy 10^{19} eV.

particles. The error ratio was 0.9998% and 0.9989%, respectively, for iron and proton as primary particles. These results are satisfactory. We can consider that the sigmoidal function (logistic model) applies well both to iron and protons.

4. Conclusions

The simulation of EAS lateral distribution function was performed by using AIRES system for three hadronic interaction models (SIBYLL, QGSJET, and EPOS) for iron nuclei and protons primaries. In addition, the simulation was performed for three different high energies 10^{17} , 10^{18} and 10^{19} eV and two zenith angles 0° and 10° of several secondary particles. In addition, the parameters of LDF were calculated as a function of the primary energy, using the results of the simulation, through the sigmoidal function (logistic model) for the primary protons as well as iron nuclei within the energy range 10^{17} – 10^{19} eV. We obtained the new function $K(E)$ by developing a sigmoidal function that depends on four parameters as a function of the primary energy. The comparison of the parameterized lateral distribution function with that measured with the AGASA observatory demonstrates the ability to classify and calculate the energies of

primary particles and determining around the CR energy spectrum and a region of angles. The results differ from those available in the literature as to develop the sigmoid function as a function of the primary energy. The ability to build a library of lateral distribution samples that could be used for analyzing specific events observed with the EAS array and reconstruction of the primary CRs energy spectrum as well mass composition is the key benefit of the current method.

Acknowledgments

Authors thank Mustansiriyah University in Baghdad Iraq (see uomustansiriyah.edu.iq) and AIRES system creators for their support in this work.

References

- [1] A.N. Cillis, S.J. Sciutto, *Phys. Rev. D* **64**, 013010 (2001).
- [2] E.M. Holt, *J. Phys. Conf. Ser.* **718**, 052019 (2016).
- [3] A. Aab, P. Abreu, M. Aglietta et al., *J. Cosmol. Astropart. Phys.* **2019**, 022 (2019).
- [4] K.F. Fadhel, A.A. Al-Rubaiee, H.A. Jassim, I.T. Al-Alawy, *J. Phys. Conf. Ser.* **1879**, 032089 (2021).
- [5] S.P. Knurenko, A.A. Ivanov, M.P. Pravdin, A.V. Sabourov, I.Y. Slepsov, *Nucl. Phys. B Proc. Suppl.* **175-176**, 201 (2008).
- [6] M. Roth for the Auger Collaboration, in: *Proc. 28th ICRC, Tsukuba (Japan)*, arXiv:astro-ph/0308392, 2003.
- [7] M.W. Friedlander in: *A Thin Cosmic Rain*, Harvard University Press, London 2013, p. 117.
- [8] S.J. Sciutto, *Proc. of 27th ICRC, Hamburg (Germany)*, arXiv:astro-ph/0106044, 2001, p. 2.
- [9] A.A. Lagutin, R.I. Raikin, N. Inoue, A. Misaki, *J. Phys. G Nucl. Part. Phys.* **28**, 1259 (2002).
- [10] A.A. Ivanov, *Proc. Sci.* **301**, 550 (2017).
- [11] A.A. Lagutin R.I. Raikin, *Nucl. Phys. B Proc. Suppl.* **97**, 274 (2001).
- [12] D. Barnhill, P. Bauleo, M.T. Dova et al., for the Pierre Auger Collaboration, *Proceedings of 29th ICRC, Pune (India)*, arXiv:astro-ph/0507590, 2005, p. 101.
- [13] KASCADE Collaboration T. Antoni et al., *Astropart. Phys.* **14**, 245 (2001).
- [14] R. Engel, D. Heck, T. Pierog, *Annu. Rev. Nucl. Part. Sci.* **61**, 467 (2011).
- [15] P. Bernardini, A. D'Amone, I. De Mitri, G. Marsella, A. Surdo, *Proc. Sci.* **236**, 388 (2016).

- [16] H.A. Jassim, A.A. Al-Rubaiee, I.T. Al-Alawy, *Indian J. Public Heal. Res. Dev.* **9**, 1307 (2018), [arXiv:2007.16004v1](#).
- [17] R. Engel, T.K. Gaisser, P. Lipari, T. Stanev, in: *Proc. 26th ICRC, Salt Lake City (UT)*, Vol. 1, 1999, p. 415.
- [18] S. Ostapchenko, *Phys. Rev. D* **83**, 014018 (2011).
- [19] T. Pierog, I. Karpenko, J.M. Katzy, E. Yatsenko, K. Werner, *Phys. Rev. C* **92**, 034906 (2015).
- [20] M. Takeda, N. Sakaki, K. Honda et al., *Astropart. Phys.* **19**, 447 (2003).